Flexible and Printed Electronics



# Printable, adhesive, and self-healing dry epidermal electrodes based on PEDOT:PSS and polyurethane diol



Flexible and Printed Electronics

PAPER

# Printable, adhesive, and self-healing dry epidermal electrodes based on PEDOT:PSS and polyurethane diol

Pierre Kateb[1], Jiaxin Fan[1], Jinsil Kim[1], Xin Zhou[1], Gregory A Lodygensky[2] and Fabio Cicoira[1,*]

[1] Department of Chemical Engineering, Polytechnique Montréal, Montreal, Canada
[2] Department of Pediatrics, CHU Sainte-Justine Research Center, University of Montréal, Montreal, Canada
* Author to whom any correspondence should be addressed.

**E-mail:** fabio.cicoira@polymtl.ca

**Keywords:** PEDOT:PSS, electrophysiology, printable electronics, stretchable bioelectronics, polyurethane

Supplementary material for this article is available online

OPEN ACCESS

RECEIVED
8 August 2023

REVISED
3 October 2023

ACCEPTED FOR PUBLICATION
23 October 2023

PUBLISHED
16 November 2023



## Abstract

Printable, self-healing, stretchable, and conductive materials have tremendous potential for the fabrication of advanced electronic devices. Poly(3,4-ethylenedioxithiopene) doped with polystyrene sulfonate (PEDOT:PSS) has been the focus of extensive research due to its tunable electrical and mechanical properties. Owing to its solution-processability and self-healing ability, PEDOT:PSS is an excellent candidate for developing printable inks. In this study, we developed printable, stretchable, dry, lightly adhesive, and self-healing materials for biomedical applications. Polyurethane diol (PUD), polyethylene glycol, and sorbitol were investigated as additives for PEDOT:PSS. In this study, we identified an optimal printable mixture obtained by adding PUD to PEDOT:PSS, which improved both the mechanical and electrical properties. PUD/PEDOT:PSS free-standing films with optimized composition showed a conductivity of approximately 30 S $cm^{-1}$, stretchability of 30%, and Young's modulus of 15 MPa. A low resistance change (<20%) was achieved when the strain was increased to 30%. Excellent electrical stability under cyclic mechanical strain, biocompatibility, and 100% electrical self-healing were also observed. The potential biomedical applications of this mixture were demonstrated by fabricating a printed epidermal electrode on a stretchable silicone substrate. The PUD/PEDOT:PSS electrodes displayed a skin-electrode impedance similar to commercially available ones, and successfully captured physiological signals. This study contributes to the development of improved customization and enhanced mechanical durability of soft electronic materials.

## 1. Introduction

The conducting polymer poly(3,4-ethylenedioxythiopene) doped with poly(styrenesulfonate) (PEDOT:PSS) is the subject of widespread research owing to its versatility in electronic and biomedical applications [1–5]. The ability to achieve enhanced electrical conductivity, stretchability, and self-healing properties upon addition of other compounds makes PEDOT:PSS attractive for electrophysiological sensors and bioelectronics. Proper adhesion on skin, mechanical properties resembling those of biological tissues, and self-healing ability are key factors in improving the reliability and prolonging the lifespan of such electronic devices. We have previously reported stretchable conductive films obtained by printing commercial PEDOT:PSS ink on thermoplastic polyurethane (PU). This method was used to develop an electrodermal activity sensor. However, ensuring optimal skin contact required a Velcro strap [6]. Another approach to promote contact with skin is to fabricate adhesive and soft PEDOT:PSS-based hydrogels. By adding poly(vinyl alcohol) (PVA), $\beta$-cyclodextrin and citric acid, Tan *et al* obtained highly stretchable (700%), conductive (1–37 S $cm^{-1}$), low modulus (56.1–401.9 kPa), and

adhesive (∼4 N $cm^{-1}$) PEDOT:PSS-based composites, which were also used to fabricate solution-processed adhesive conductive gel electrodes for soft electronics [7]. Recently, our group [8] successfully produced a self-healing, adhesive, conductive, and stretchable PEDOT:PSS-based hydrogel by mixing PVA and borax with a commercial PEDOT:PSS suspension in glycols (diethylene and propylene glycol). The use of hydrogels as materials for epidermal electrodes has also been demonstrated. Considering the potential issues of water loss in ambient environments, the development of dry adhesive conductive materials with appropriate mechanical properties presents a more viable path for long-term soft device applications [4, 9, 10]. Building on this premise, Zhang *et al* [4] combined waterborne PU and D-sorbitol with PEDOT:PSS to create highly conductive, stretchable, and adhesive films. These films could be employed as dry electrodes for capturing electrocardiography (ECG) and electromyography (EMG) signals with low noise levels and skin-electrode impedance.

PEDOT:PSS can be processed by various techniques. Specifically, there is an increasing interest in the development of printable materials with high conductivity, stretchability, and self-healing capabilities, given that printing offers a cost-effective and customizable path to mass production [11]. PEDOT:PSS is an excellent material for printable [12–17] and self-healing [5, 18–21] electronics. Su *et al* printed a stretchable self-healable channel material for organic electrochemical transistors by blending PEDOT:PSS and a soft polymer, (poly(2-acrylamido-2-methyl-1-propanesulfonic acid) [20]. Ye *et al* reported an injectable conductive self-healing hydrogel for wearable electronics with applications in healthcare, using an interpenetrating polymer network consisting of multiwalled carbon nanotubes, PEDOT:PSS, polyacrylamide, PVA and borax [21]. Excellent mechanical and electrical properties, in addition to printability, self-healing, and adhesion, were achieved using a mixture of PU and PEDOT:PSS [4, 22, 23]. PU has been extensively used in biomedical applications and has many advantages, such as biocompatibility, biodegradability, and tunable chemical and physical properties [24–26].

In this study, we employed polyurethane diol (PUD) to enhance both the stretchability (∼30%) and electrical conductivity (∼30 S $cm^{-1}$) of PEDOT:PSS and foster light adhesion (<0.04 N $cm^{-1}$) on fake skin and instilling electrical self-healing capabilities. Furthermore, the PUD with PEDOT:PSS allowed the production of a conductive polymer ink. PUD was selected owing to its water solubility, with the aim of developing sustainable conducting polymer inks. The PUD/PEDOT:PSS films exhibited tolerance to repeated strain, electrical stability under mechanical cycling, and biocompatibility. Additionally, we developed printed PUD/PEDOT:PSS epidermal electrodes on a flexible silicone substrate, with a skin-electrode impedance comparable to that of commercial Ag/AgCl gel electrodes, and stable ECG and EMG signal recording. These findings highlight the potential of PUD/PEDOT:PSS in the measurement of high-quality epidermal biopotential signals. This study paves the way for improved customizability, enhanced durability, and minimized discomfort with epidermal electrodes.

## 2. Experimental methods

### 2.1. Chemicals and materials

Polyethylene glycol (PEG) 400 and PUD were purchased from Sigma-Aldrich. An aqueous suspension of PEDOT:PSS (Clevios PH1000, PEDOT concentration of approximately 1–1.3 wt. %) was supplied by Heraeus Precious Metals. Sorbitol was purchased from Caledon Laboratories Ltd The stretchable silver ink, used to print the metal contacts for the electrodes was donated by Chimet S.p.A (Italy). A silicone elastomer kit (SYLGARD® 184), Dow Corning (USA), was used to prepare polydimethylsiloxane (PDMS). Polybutylene adipate terephthalate (Ecoflex Gel), used as the adhesive layer, was purchased from Smooth-On (USA). S mm flange (14SF-9 STUD-SS) and eyelets for studs (11 EYELET-R-NIC), were purchased from Rome Fastener Corporation (USA). A silicone-based 'fake skin' with softness and stretchability similar to those of human skin was purchased from PIXESTT on Amazon. For the biocompatibility test, the C2C12 muscular mouse cell line was purchased from ATCC (USA). Dulbecco's phosphate-buffered saline (DPBS) powder, without magnesium or calcium was purchased from Gibco. Nunc™ Nunclon Delta-treated flat-bottom 96-well plates from Thermo Fisher Scientific (USA) and OptiPlateTM-96 Black (Perkin Elmer, USA) were used for cell culture. The LIVE/DEAD Viability/Cytotoxicity Kit for Mammalian Cells (calcein AM/ethidium homodimer assay) was supplied by Thermo Fisher Scientific.

### 2.2. Preparation of thin films and epidermal electrodes

*2.2.1. Free-standing films*

To understand the influence of each component on the adhesion, electrical, mechanical, and self-healing properties, 12 different mixtures of PEDOT:PSS, PUD, PEG, and sorbitol were prepared. Their compositions are listed in table 1. The chemical structures of the materials are shown in figure 1(a).

**Table 1.** Composition of the different PEDOT:PSS mixtures for electrical and mechanical characterizations.

| PUD (wt%) | PEG (wt%) | Sorbitol (wt%) | PH1000 (wt%) |
|---|---|---|---|
| 2 | 0 | 0 | 98 |
| 5 | 0 | 0 | 95 |
| 10 | 0 | 0 | 90 |
| 0 | 2 | 0 | 98 |
| 2 | 2 | 0 | 96 |
| 5 | 2 | 0 | 93 |
| 0 | 5 | 0 | 95 |
| 0 | 0 | 2 | 98 |
| 2 | 0 | 2 | 96 |
| 5 | 0 | 2 | 93 |
| 0 | 0 | 5 | 95 |
| 0 | 0 | 0 | 100 |

Each mixture was stirred in a sealed vial at 1000 rpm using a magnetic stirrer for 30 min on a hot plate at 160 °C. Then, 2 g of the solution were poured into a 40 mm × 55 mm × 1 mm polymethylmethacrylate (PMMA) mold and heated at 70 °C for 4 h in an oven to remove water and obtain a dry film. This heating temperature was chosen to avoid damaging the mold (PMMA softens above 80 °C) and deteriorating the mechanical properties of the films, which are sensitive to high temperature treatments. The obtained films were cut using a razor blade into 10 mm × 40 mm strips, which were used for electrical and mechanical characterization.

*2.2.2. Epidermal electrodes*

The stretchable substrate were prepared by pouring PDMS base and curing agent (10:1) into a PMMA mold, degassing for 1 h to remove air bubbles and curing at 70 °C in an oven for 4 h. Ecoflex was drop-cast over the PDMS, degassed, and cured at room temperature for 4 h. This procedure yielded 1 mm thick double-layered stretchable substrates, where the Ecoflex side was lightly adhesive, and the PDMS substrate was non-adhesive. The non-tacky PDMS layer facilitated the demolding of the adhesive Ecoflex gel and acted as a carrier substrate for the entire structure, enhancing overall handling. Electrodes were printed on the adhesive side.

To prepare the PUD/PEDOT:PSS ink, a solution of PEDOT:PSS with 5% PUD, selected for electrode experiments, was heated to remove 50% by weight of the water, to obtain the higher viscosity required for printing. The resulting ink was filtered using a Chromspec UV syringe filter (25 mm diameter and 5 $\mu$m pore size) to remove large particles.

Using a printed circuit board printer (Voltera V-One, Canada), a layer of stretchable silver was first printed on the Ecoflex/PDMS substrate as the metal contact and cured at 50 °C for 15 min. The silver layer was not fully cured in this step, as it was also heated after printing the PEDOT:PSS layer. The PUD/PEDOT:PSS ink was printed on top of stretchable silver to form the active part of the electrode (diameter of 19 mm) and heated at 80 °C for 120 min. Finally, snap buttons were installed using a Benchtop Model RFC03 (Rome Fastener Corporation, USA) to connect the electrodes to the ECG, EMG and skin-electrode impedance characterization devices.

### 2.3. Characterization and measurements

*2.3.1. Mechanical, electrical, and electromechanical testing*

For each mixture listed in table 1, three different films with a width of 10 mm, a distance between grips of 10 mm, and different thicknesses listed in table S1 were used for the mechanical characterization. A Mach-1 V500csst MA009 instrument, Biomomentum Inc. (Canada), was used for tensile, electro-tensile and adhesion measurements. The thickness used to calculate the conductivity and Young's modulus was measured with Mach-1 Biomomentum using an indenter with a 1 mm diameter tip. A 70 N and 1.5 N load cells were used in a uniaxial strain at a ramp rate of 1 mm min$^{-1}$. The load cell was calibrated prior to each use. The ramp rate and number of samples were set according to the American Society for Testing and Materials (ASTM) 882 standard [27]. A four-point probe configuration was used to measure the variation in resistance during tensile testing using a Keysight B2902A. This same system was used to measure the initial resistance of films at different voltages, and the conductivity was calculated using Ohm's law:

$$\sigma = \frac{L}{R \cdot A}$$

where $\sigma$ is the conductivity, $L$ is the sample length, $R$ is the measured resistance, and $A$ is the sample cross-sectional area. To test the resistance change under cyclic stretching and strain-stress testing, the measured resistances were normalized as $R/R0$, where $R0$ is the initial resistance measured before the mechanical tests.

The adhesion force was measured following the standard test method for 90 degree peel resistance of adhesives, ASTM D6862 [28]. A free-standing PEDOT:PSS-based rectangular film of 65 mm × 10 mm was adhered onto glass or fake skin and then peeled at an angle of 90° between the substrate and the film and a rate of 50 mm min$^{-1}$ for a length of 5 cm. The same test was repeated three times for each PEDOT:PSS-based mixture, and the error bars represent the standard deviation. The same test was performed for the Ecoflex/PDMS substrate, using the Ecoflex as the adhesive side, to get a reference value for the adhesion force.

*2.3.2. Thermogravimetric analysis (TGA)*

TGA was performed using a TG Q500 (TA Instruments, USA) to estimate the water content and understand the interactions between the PUD and PEDOT:PSS. Three samples were used: 5 wt % PUD, pristine PEDOT:PSS, and pristine PUD. The 5% PUD/PEDOT:PSS and pristine PEDOT:PSS films were prepared using the heating conditions described earlier, and the pristine PUD sample was heated overnight at 100 °C to remove the solvent. Each dried sample (10 mg) was analyzed in a platinum pan over a temperature range of 40 °C–800 °C (heating rate of 10 °C $min^{-1}$) under nitrogen atmosphere (flow rate of 60 ml $min^{-1}$).

*2.3.3. Fourier transform infrared spectrophotometry (FTIR)*

The IR spectra of the films were collected with a Perkin Elmer FTIR Spectrum 65 for a range of 600–4000 $cm^{-1}$ at a resolution of 4 $cm^{-1}$ for 16 scans.

### 2.4. Electrical self-healing measurements

Self-healing measurements were performed on free-standing (5% PUD/PEDOT:PSS, 5% PEG/PEDOT:PSS, and 5% sorbitol/PEDOT:PSS) and printed (5% PUD/PEDOT:PSS) films with dimensions of 10 mm × 40 mm. The free-standing films were placed on a microscope glass slide whereas the printed films were directly printed on glass. Two tungsten probes (Imina Technologies, Switzerland) placed at the two ends of the film were used to establish electrical contacts. A constant voltage (0.2 V) was applied to the film using a Keysight B2902A source/measurement unit, and the electrical current was continuously monitored during the process. For the 5% sorbitol/PEDOT:PSS film, which exhibited low conductivity (table S3), an applied voltage of 2 V was used for the self-healing tests. The cuts were manually created using a razor blade (Ultrasource Single Edge blade 500 205), yielding a size of approximately 20 $\mu$m. Multiple cuts were made at various locations on the films. Each cut was made after the current was stabilized. All experiments were carried out under ambient conditions.

### 2.5. Biocompatibility

Cell culture was performed by seeding C2C12 cells (mouse muscle cells) on PEDOT:PSS-coated 96-wells. Approximately 5 $\mu$l of 5% PUD/PEDOT:PSS solution was used to coat a 96-well plate, which was subsequently dried under sterile conditions and then washed with DPBS to remove residues. To quantify the viability of the cells on the PUD/PEDOT:PSS, a live/dead calcein-AM/ethidium homodimer (EthD-1) assay was performed after 3 and 5 d. Black 96-well microplates were used for fluorescence measurements with a Tecan Infinite 200 Pro microplate reader (Switzerland) at excitation/emission wavelengths of 494/517 nm and 528/617 nm for calcein and EthD-1, respectively. For the fluorescence microscope, the images were acquired using GFP and Texas Red EVOS light cube filters for calcein and EthD-1, respectively, with an EVOS M5000 Invitrogen inverted benchtop microscope (USA).

### 2.6. Biopotential and skin-electrode impedance measurements

For biopotential and skin-electrode impedance measurements, we followed previously used protocols [8, 17]. The OpenBCI Cyton device was used to measure the ECG and EMG signals at a sample rate of 250 Hz. For ECG, the electrodes were placed on the left and right arms, and the reference electrode was placed on the right leg. A band-pass filter from 5 to 50 Hz, notch filter at 60 Hz, and gain of 24 were used. Signal baseline correction and the ECG complexes superposition were performed using an open-source Python toolbox for physiological signals, neurokit2 [29]. Using the python toolbox, the *R* peaks of PQRST complexes of an ECG signal are identified. Subsequently, each complex is delineated and superposed by aligning the *R* peaks, and the PQST peaks are identified. For the EMG measurements, the active electrodes were placed on the right bicep, 5 cm apart, and the reference on the elbow of the volunteer. The signals were recorded as the volunteer contracted the right bicep muscle by flexing it, without performing any specific exercise or movement. A band-pass filter of 15–50 Hz was used and the signal was post-processed for baseline correction using the Python toolbox BioSPPy [30].

The skin-electrode impedance was measured using an electrochemical workstation (VSP-300, BioLogic, France) and a setup of three electrodes (working, reference, and counter electrodes) placed linearly on the forearm of a volunteer, at 6 and 12 cm from the first electrode. A PUD/PEDOT:PSS composite electrode (diameter of 19 mm) was used as the working electrode, while two commercial dry Ag/AgCl silicone gel electrodes (Natus, diameter of 19 mm) were used as the reference and counter electrodes.

The skin-electrode impedance was measured from 1 Hz to 100 kHz at 10 mV. All skin-electrode impedance measurements were collected from a single volunteer, a 24 year-old light-skinned male, at the same location and on the same day.

## 3. Results and discussion

### 3.1. Film and electrode fabrication

Epidermal electrophysiological electrodes require adhesion on skin, a suitable Young's modulus, stretchability, and low impedance at the skin interface for reliable signal transmission. We opted for

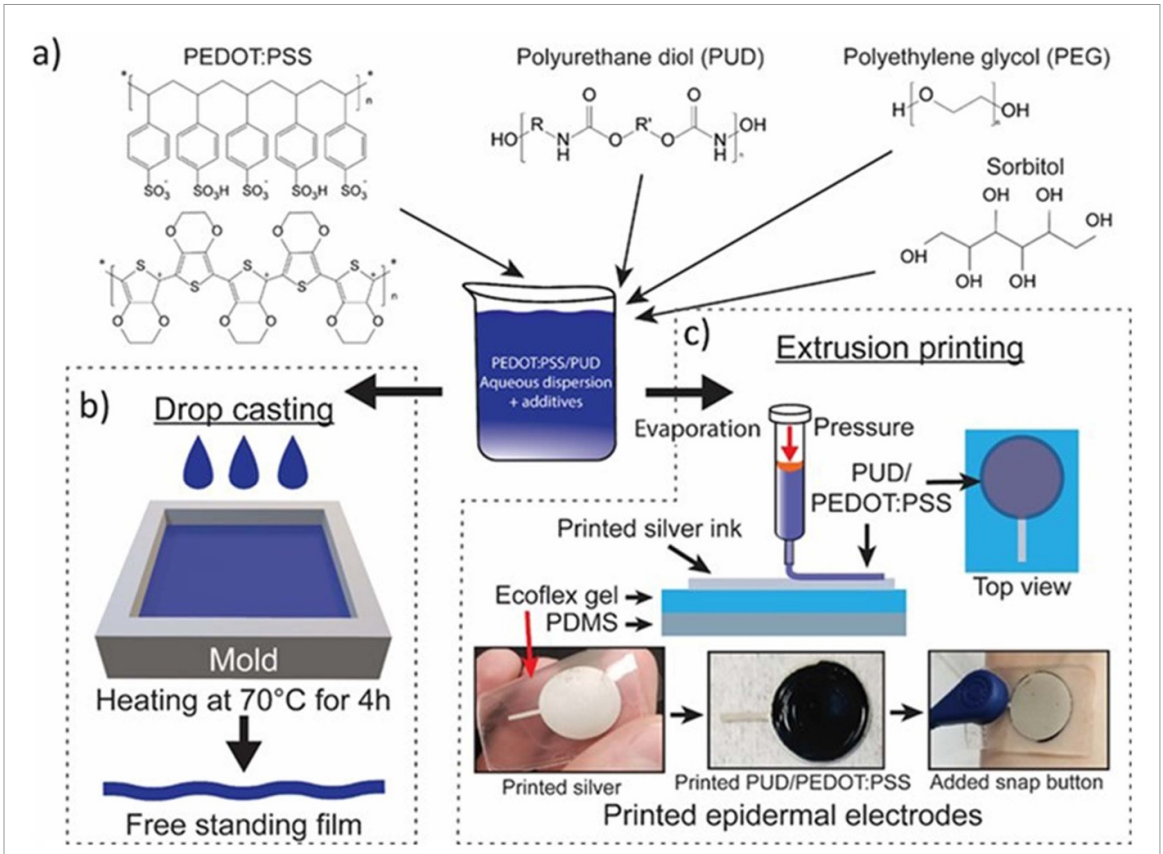


**Figure 1.** Schematic illustration of the fabrication process. (a) Chemical structures of PEDOT:PSS, PUD, PEG, and sorbitol. (b) Free-standing film preparation by drop casting the different PEDOT:PSS based mixtures listed in table 1 in a PMMA mold. (c) Printing of the PUD/PEDOT:PSS based epidermal electrode on PDMS/Ecoflex substrate. Photographs of printed silver contact, PUD/PEDOT:PSS printed on top of silver, and complete epidermal electrode with snap button added.

PEDOT:PSS as the electrode material because of its tunable electrical conductivity and mechanical properties, which can be achieved upon mixing with other materials. PUD, PEG, and sorbitol were mixed with PEDOT:PSS to investigate their impact on the electrical and mechanical properties and to achieve optimal adhesion, stretchability, electrical conductivity, self-healing performance, and biocompatibility. PEG has previously been used to enhance the conductivity of PEDOT:PSS films and their self-healing properties, with an effect on their Young's modulus and elongation at break [31], whereas sorbitol is recognized to improve conductivity, adhesion and stretchability [4, 32]. We combined these three additives with PEDOT:PSS, to improve both the mechanical and electrical properties. Free-standing films (figure 1(b)) were prepared to assess the material properties. Electrophysiological electrodes were subsequently printed using the optimized formulation (figure 1(c)). Our epidermal electrode consists of an elastic Ecoflex/PDMS substrate, electrical interconnects based on stretchable silver ink, and a PUD/PEDOT:PSS top layer.

### 3.2. Mechanical characterization

To facilitate painless removal of the electrodes from the skin, we targeted an adhesion comparable to that of Ecoflex [10, 33], which showed an average adhesion force of 0.045 N $cm^{-1}$ on fake skin (figure 2(a) and table S2). Painless removal of adhesive was observed in clinical research for up to ~0.5 N $cm^{-1}$ [34, 35]. The pristine PEDOT:PSS and the 2% PUD/PEDOT:PSS films did not adhere to the glass or fake skin. The 5% PUD/PEDOT:PSS, 10% PUD/PEDOT:PSS, 2% sorbitol/2%PUD/PEDOT:PSS, and 2%PUD/5%sorbitol/PEDOT:PSS films demonstrated an adhesion on fake skin similar to that of the Ecoflex gel (figure 2(a)). This indicates that adding enough PUD and sorbitol improved the adhesion of the films. However, as the 10% PUD/PEDOT:PSS films had a viscous residue on their surface after drying due to excess PUD, they were not considered further. While the addition of PEG significantly improved the conductivity, the films exhibited weak adhesion on both glass and fake skin making them unsuitable for adhesive epidermal electrodes.

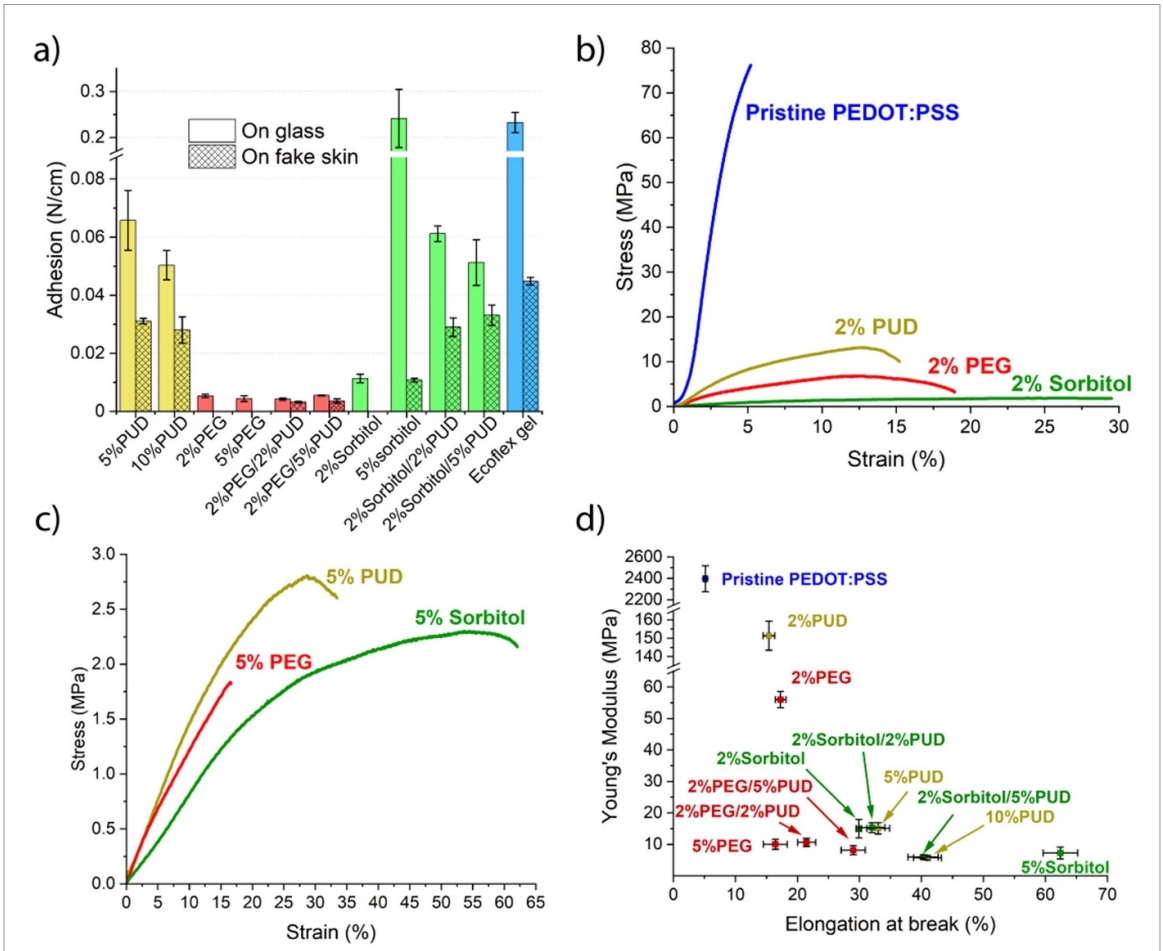


**Figure 2.** (a) Adhesion on glass and on fake skin for different compositions of PEDOT:PSS-based films and the Ecoflex gel ($n = 3$). Strain–stress curves of PEDOT:PSS with (b) low percentage additives (pristine PEDOT:PSS, 2% PUD, 2% PEG and 2% sorbitol) and (c) 5% PUD, 5% PEG and 5% sorbitol. (d) Relationship between Young's modulus and elongation at break for different compositions of PEDOT:PSS-based films ($n = 3$).

Stretchability and Young's moduli similar to those of the skin are crucial characteristics for epidermal electrodes to maintain proper contact with the skin, prevent irritation, and ensure the comfort of the wearer [36]. The Young's modulus of human skin can range from 5 kPa to 140 MPa (depending on whether it is measured by indentation in the thickness direction for a lower modulus or by tensile testing for a higher modulus) [37]. Therefore, we studied the mechanical properties of the films with different compositions. The strain–stress curves in figure 2(b) refer to films made of pristine PEDOT:PSS and its mixtures with 2% PUD, PEG, or sorbitol. Figure 2(c) depicts the strain-stress curves for PEDOT:PSS films with 5% PUD, PEG and sorbitol.

Our results unequivocally show that adding PUD, PEG and sorbitol to PEDOT:PSS leads to films with larger elongations at break and lower Young's moduli than pristine PEDOT:PSS (figure 2(d), table S3). The most stretchable films (up to 66%) were obtained for 10% PUD/PEDOT:PSS, 5% sorbitol/PEDOT:PSS, and 2% sorbitol/5% PUD/PEDOT:PSS. The addition of sorbitol had the most significant effect on the stretchability of PEDOT:PSS films. The addition of PUD to sorbitol/PEDOT:PSS further improved the stretchability of the film. Increasing the amount of PEG was effective in reducing the Young's modulus; however, the elongation remained almost identical for samples with 2% and 5% PEG. Nonetheless, a significant improvement in stretchability was observed when adding 5% PUD to 2% PEG films. This effect can be attributed to the formation of hydrogen bonds between the additives and PSS, which decreases the interactions between PEDOT and PSS chains and leads to an increase of the free volume between polymer chains [38, 39]. The ensuing chain separation and uncoiling of PEDOT:PSS reduce the distance between the conductive PEDOT chains, thereby improving the conductivity of the resulting polymer blend [40, 41]. We hypothesize that water-soluble PUD exerts comparable effects

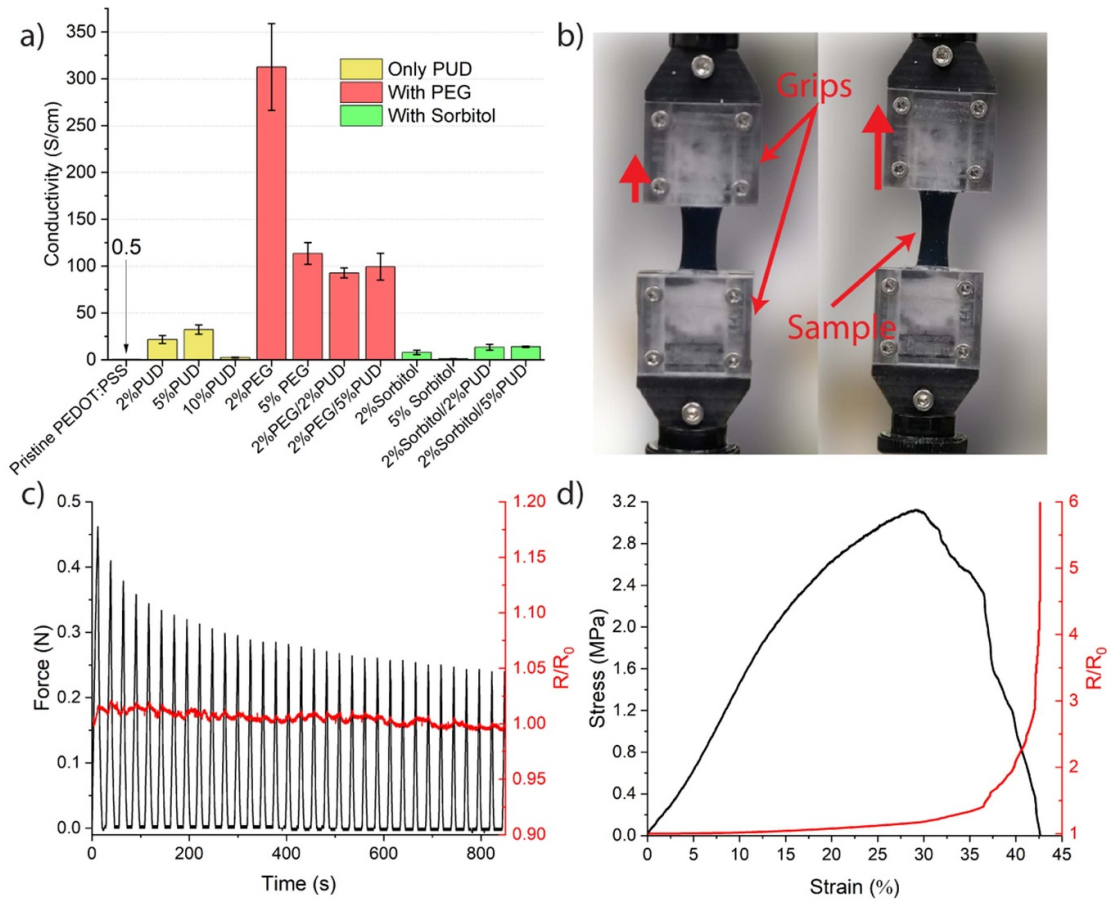


**Figure 3.** (a) Conductivities of films based on different PEDOT:PSS formulations. ($n = 3$) (b) Photograph of the electromechanical measurement setup with grips, sample, and stretching direction. (c) Resistance variation vs time of the 5% PUD/PEDOT:PSS film when cyclically stretched 10% of the initial length. (d) Resistance change of the 5% PUD/PEDOT:PSS film when stretched until break.

on improving film stretchability and conductivity. To further assess the stability of PEDOT:PSS-based films over time, three types of samples (5% PUD/PEDOT:PSS, 5% PEG/PEDOT:PSS, and 5% sorbitol/PEDOT:PSS) were stored under ambient conditions for a week, and then their mechanical properties were characterized (table S5). The mechanical properties of 5% PEG/PEDOT:PSS films remained virtually unchanged. 5% PUD/PEDOT:PSS films exhibited an approximately 55% increase in their Young's modulus and around 30% decrease in elongation at break. The 5% sorbitol/PEDOT:PSS films demonstrated the most significant deterioration, becoming brittle, with their Young's modulus increasing more than 20-fold and their elongation at break decreasing to about 10% of its original value. These alterations can be traced back to the loss of additives and slow water evaporation following the initial heating step. We then further examined the change in the electrical properties of the 5% PUD/PEDOT:PSS samples, as they exhibited minimal changes in their mechanical properties. Following a storage period of 5 days under ambient conditions, we observed no significant variation in conductivity (less than 5%, maintaining a range of $35 \pm 1$–$37 \pm 1$ S cm$^{-1}$). Hence, the samples prepared from the 5% PUD/PEDOT:PSS formulation preserve both their mechanical and electrical properties for at least 5 d. Therefore, these preliminary findings suggest that this material holds promise for wearable electronics applications that require measurements over extended periods of time.

### 3.3. Electrical characterization

We subsequently investigated the electrical properties of the different films. The pristine PEDOT:PSS film exhibited an average conductivity of approximately 0.5 S cm$^{-1}$, which increased upon the addition of low percentages of plasticizers (figure 3(a), table S3). The 2% PEG/PEDOT:PSS film demonstrated the highest conductivity with an average of about 300 S cm$^{-1}$, consistent with previously reported data for PEDOT:PSS film with 1% PEG [31]. Incorporation of 2% sorbitol yielded an average conductivity of about 8 S cm$^{-1}$ while increasing the concentration to 5% sorbitol decreased the

conductivity to around 1 S $cm^{-1}$. In contrast, 5% PUD/PEDOT:PSS resulted in an average conductivity of approximately 30 S $cm^{-1}$, and increasing the PUD content to 10% decreased the conductivity to around 2.5 S $cm^{-1}$. Blending 2% PEG with 5% PUD increased the conductivity to approximately 100 S $cm^{-1}$ and simultaneously improved the stretchability compared to 2% PEG alone. Nonetheless, after a certain amount of additive was incorporated into PEDOT:PSS, the electrical conductivity decreased. Among the selected additives, sorbitol resulted in the smallest conductivity enhancement. This may be attributed to the low heating temperature (70 °C) used during film preparation [32]. After heating the sorbitol/PUD/PEDOT:PSS films at 160 °C for 15 s, a significant improvement of the conductivity was observed (table S4). However, this process led to a decline in the stretchability and adhesion of the films, rendering them unsuitable for use as epidermal electrodes. As a result, 70 °C was selected as the optimal temperature to remove water and obtain films.

Finally, to evaluate their resilience when exposed to water or sweat, the samples were submerged in water. The 5% sorbitol/PEDOT:PSS film completely dissolved, whereas the PEDOT:PSS films containing 5% PUD and 5% PEG remained undamaged (figure S1).

Considering their adhesion, mechanical, and electrical properties, 5% PUD/PEDOT:PSS films have emerged as the most promising candidates for fabricating epidermal electrodes. They exhibited superior conductivity than films with sorbitol and enhanced elongation compared to PEG films. Consequently, we selected these films for the electromechanical testing. To characterize the electrical stability under mechanical strain, we subjected the 5% PUD/PEDOT:PSS films to a series of cyclic strains—up to 10% of their initial length—to remain within the elastic domain of the material. The film demonstrated excellent stability under repeated stretching, with a resistance variation below 2%, as shown in figure 3(c). The change of resistance with uniaxial deformation is shown in figure 3(d). The resistance rose by less than 20% before the onset of breaking, after which it increased by over 100% when the film started breaking around 30% strain mark (figure 3(d)). These findings substantiate the excellent electrical stability of PUD/PEDOT:PSS films under moderate strains, suggesting that they can mimic the stretchability of the skin without notably compromising the conductivity of the electrode. Furthermore, ideal materials for wearable electronics should be resilient to physical damage and possess the capacity to mend minor cracks when subjected to mechanical injuries, such as cuts. In an effort to evaluate whether our PEDOT:PSS-based films exhibit this property, a 5% PUD/PEDOT:PSS free-standing film was completely cut using a razor blade while monitoring the current under constant voltage. As depicted in figure 4(a), upon the complete separation of the film, the current dropped to the noise level, indicative of interrupted electrical conduction. Immediately after the cut, the two parts autonomously came into contact, leveraging the intrinsic self-healing nature of the PUD/PEDOT:PSS film (movie S1), and the current was restored to ∼100% of its initial level. We repeated this process several times on the same film and consistently witnessed this behavior. The self-healing ability of 5% PEG/PEDOT:PSS and 5% sorbitol/PEDOT:PSS films were also examined (figure S2). The free-standing 5% PEG/PEDOT:PSS film showed no significant decrease in current when cut, but the current was noisier than the other types of samples. Although the 5% sorbitol/PEDOT:PSS film nearly fully recovered after the initial two cuts, subsequent cuts led to only partial recovery. Thus, 5% PUD/PEDOT:PSS film demonstrated superior electrical self-healing behavior compared to its counterparts. The same test was performed on a printed 5% PUD/PEDOT:PSS film which also revealed consistent electrical self-healing (figure 4(b)). This self-healing ability aligns with findings from other studies examining PEDOT:PSS-based self-healing materials with other additives [18, 31, 42]. The manual nature and individual variations of the cuts as well as a prior imperfect cut may account for slower and reduced current recovery after the 4th cut on the printed sample. Additionally, while the free-standing film is placed on a glass slide, the printed film is directly cured on glass. This may reduce film mobility and account for its slower recovery. Figures 4(c)–(f) provide microscope images of the 5% PUD/PEDOT:PSS film before and after damage, as well as during its recovery.

The integration of plasticizers or other polymers, such as PUD, into PEDOT:PSS leads to electrical self-healing, which is achieved through reduced polymer film crystallinity, increased viscoelasticity, and decreased Young's moduli [42]. Furthermore, $\pi$–$\pi$ interactions between the aromatic groups of PEDOT:PSS and hydrogen bonds between the urethane groups on PUD and sulfonate groups on PSS likely improve the self-healing ability of the PUD/PEDOT:PSS composite [42]. Owing to its high electrical conductivity, suitable stretchability, adequate adhesion, and consistent electrical self-healing behavior, we selected 5% PUD/PEDOT:PSS for fabricating epidermal electrodes.

### 3.4. Physico-chemical characterization

Since the 5% PUD/PEDOT:PSS demonstrated the most appealing properties for epidermal electrodes, we conducted both TGA and FTIR measurements on pristine PEDOT:PSS, pristine PUD, and a 5%

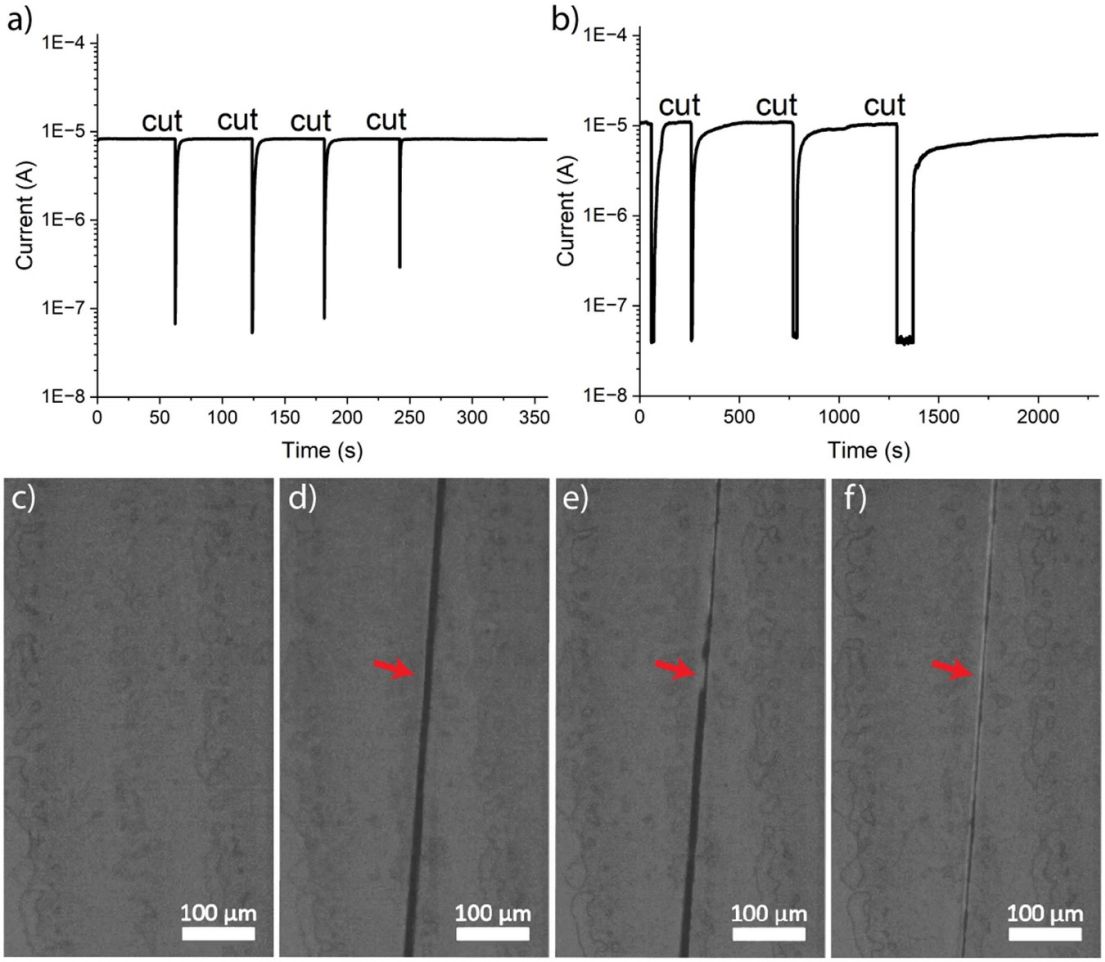


**Figure 4.** Current vs time plot showing repeated electrically self-healing of (a) drop-cast and (b) printed 5% PUD/PEDOT:PSS films for four cuts at different locations. Optical microscopic images of a 5% PUD/PEDOT:PSS free-standing film on glass (c) before damage, (d) after cutting with a razor blade, (e) partially healed, and (f) fully healed approximately 5 s after the cut.

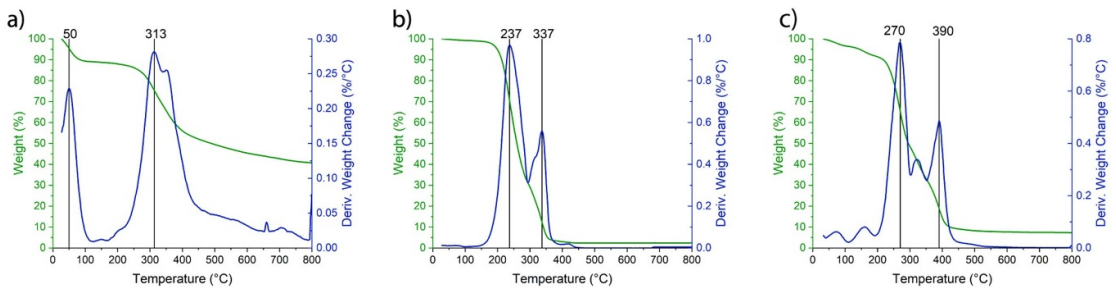


**Figure 5.** Thermogravimetry (TGA) and derivative thermogravimetry (DTG) curves of dried (a) pristine PEDOT:PSS, (b) pristine PUD, and (c) PEDOT:PSS with 5% PUD.

PUD/PEDOT:PSS film. These tests allowed us to confirm the enduring presence of PUD in the film post-processing, investigate the water content of the film, and delve deeper into the interaction between PEDOT:PSS and PUD.

The pristine PEDOT:PSS film contained about 10 wt% water, as approximately 10% weight loss was observed when the sample was heated to 100 °C (figure 5(a)). Conversely, the fully dried PUD sample revealed no residual water (figure 5(b)). As shown in figure 5(c), the 5% PUD/PEDOT:PSS sample contains about 5% water, qualifying it as a dry electrode.

Due to their low water content, especially when compared to wet electrodes such as hydrogel-based alternatives, dry electrodes tend to be more durable over time as their functionality remains unaffected by water loss. Hydrogel-based epidermal electrodes suffer from water evaporation at room temperature in a short period of time, leading to reduced signal recording quality and increased impedance at the

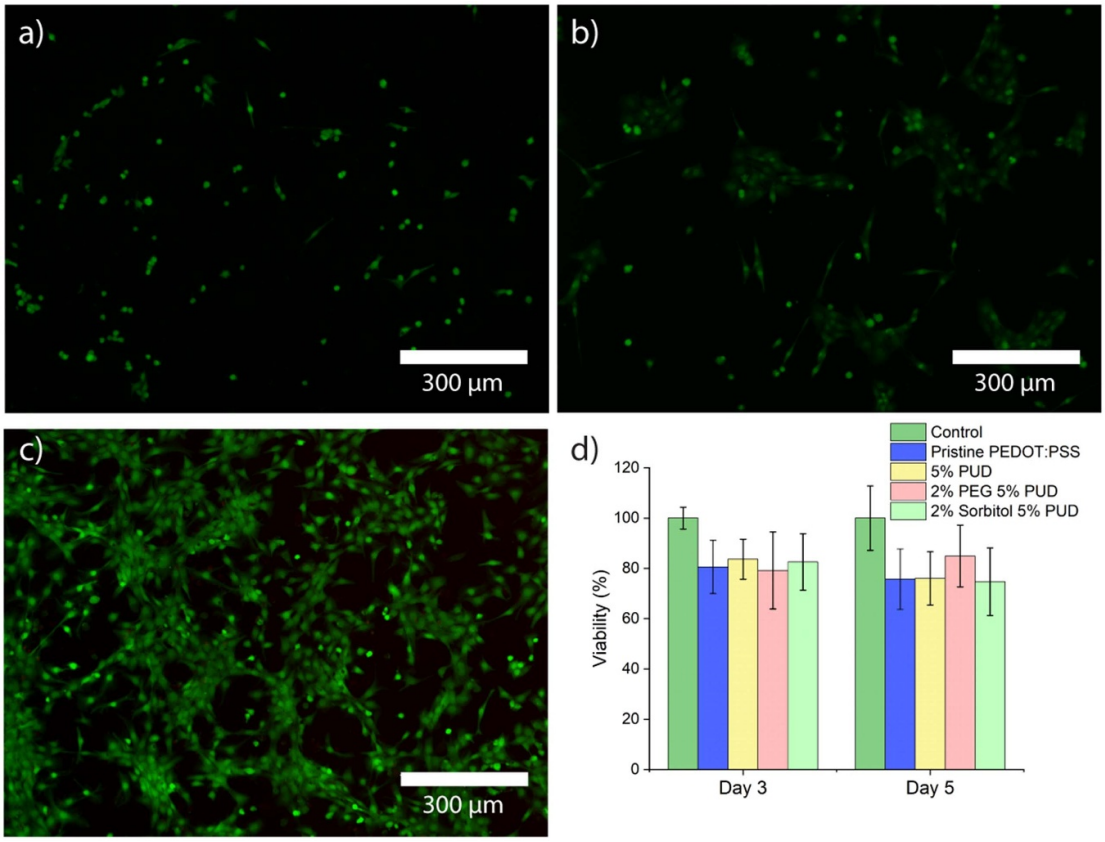


**Figure 6.** Seeded C2C12 cells on 5% PUD/PEDOT:PSS coating after (a) 1 d, (b) 3 d, and (c) 5 d. Scale bar is 300 $\mu$m. (d) Viability of cells on pristine PEDOT:PSS, 5% PUD/PEDOT: PSS, 2% PEG/5% PUD/PEDOT:PSS, and 2% sorbitol/5% PUD/PEDOT:PSS compared to the control collected on day 3 and 5 ($n = 3$).

skin-electrode interface. As such, a low water content is a clear advantage for the long-term use of functional epidermal electrodes. The modest water content in PEDOT:PSS-based films can be attributed to the inherent moisture retention ability of PEDOT:PSS [43].

Furthermore, the DTG peaks for the 5% PUD/PEDOT:PSS film moved towards higher temperatures compared to pristine PEDOT:PSS and pristine PUD samples. This shift provides qualitative support for the presence of hydrogen bonds [44] between PEDOT:PSS and PUD. For pristine PEDOT:PSS, the pyrolysis peak resides around 313 °C (figure 5(a)), whereas there are two peaks for pristine PUD: one at 237 °C and the second at 337 °C (figure 5(b)). The thermal degradation of 5% PUD/PEDOT:PSS mirrored the pristine PUD, occurring in two pyrolysis stages. However, unlike the pristine PUD sample, a shift towards higher pyrolysis temperatures at 270 °C and 390 °C was measured (figure 5(c)). The DTG curves of 2% sorbitol/5% PUD/PEDOT:PSS and 2%PEG/5% PUD/PEDOT:PSS also exhibited a shift towards higher pyrolysis temperatures (figures S3(a) and (b)) when compared to the pristine PEDOT:PSS and PUD samples.

Figure S4(a) displays the FTIR spectra for pristine PEDOT:PSS, pristine PUD, and 5% PUD/PEDOT:PSS, while the FTIR spectra of PEDOT:PSS samples containing PUD, PEG and sorbitol are shown in figure S4(b). For pristine PUD and 5% PUD/PEDOT:PSS samples, characteristic peaks were observed at 3318 $cm^{-1}$ for the -NH stretching of the urethane component in PUD, 2933 $cm^{-1}$ for the -CH stretching of alkanes in PUD, and 1684 $cm^{-1}$ for the C=O stretching of the urethane component. These observations confirmed the presence of PUD in the final 5%PUD/PEDOT:PSS film.

### 3.5. Biocompatibility

To assess the biocompatibility of our PEDOT:PSS formulations, C2C12 mouse muscle cells were attached to and cultured on thin coatings of 5% PUD/PEDOT:PSS. The cells were stained with calcein AM to show intracellular esterase activity in live cells with green fluorescence and EthD-1 for dead or dying cells with damaged membranes with red fluorescence. After one day of culture, some cells appeared attached to the surface, adopting a flattened shape, whereas others were still round and not fully attached (figure 6(a)). After 3 d, the majority of the cells had adhered, and the population had

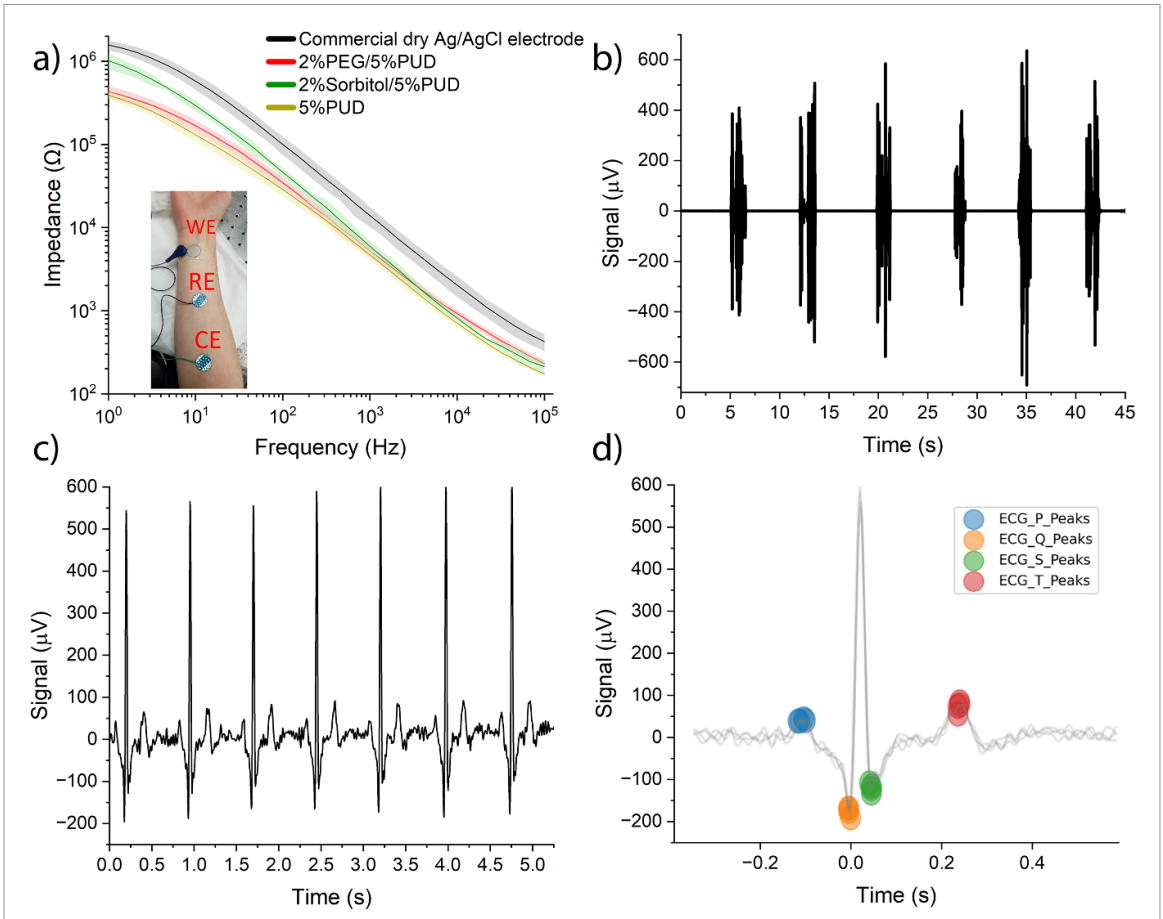


**Figure 7.** (a) Skin-electrode impedance of commercial electrode and PEDOT:PSS based electrodes with 2% PEG/5% PUD, 2% sorbitol/5% PUD, and 5% PUD ($n = 3$), and photo of the impedance measurement configuration with working (WE), reference (RE) and counter (CE) electrodes identified (inset). The shaded area around each curve represents their respective standard deviations. (b) Electromyogram (EMG) for biceps muscle and (c) electrocardiogram (ECG) signals measured using printed 5% PUD/PEDOT:PSS electrodes. (d) Delineated ECG complexes from previous graph with identifiable relevant peaks.

expanded (figure 6(b)). By day-5, the cells were confluent with only a few cells showing signs of apoptosis (figure 6(c)). The viability of cells for day 3 and 5 was confirmed using fluorescence measurements through a microplate reader. These results were compared to uncoated polystyrene wells which served as positive controls (figure 6(d)). As there is no significant difference between pristine PEDOT:PSS and PEDOT:PSS with 5%PUD, we can conclude that PUD does not significantly affect the viability. From observations during the cell culture, the ∼20% decrease between the positive control and the tested samples might be attributed to the decreased adhesion of cells on PEDOT:PSS and their slower growth. The cell viability could potentially be increased by first allowing the cells to freely adhere to the uncoated surface, and subsequently add the tested mixture and observe the growth of cells. In accordance with ISO10993-5, as the average relative viability for PEDOT:PSS films containing PUD is higher than 70% of the control group, they are considered non-cytotoxic [45]. Moreover, the viability of PEDOT:PSS with 5% PUD did not significantly deviate from that of PEDOT:PSS alone or in combination with PEG or sorbitol. Hence, the addition of up to 5% PUD did not affect the biocompatibility of PEDOT:PSS films.

### 3.6. Electrophysiological measurements

We next examined the performance of 5% PUD/PEDOT:PSS films printed on an Ecoflex Gel/PDMS substrate to evaluate their performance as epidermal electrodes for electrophysiological signal collection. The measurement setup is shown in the inset of figure 7(a). Skin-electrode impedance measurements revealed that the printed 5% PUD/PEDOT:PSS electrodes on the Ecoflex substrate had slightly lower impedance, exhibiting comparable performance to commercial electrodes (figure 7(a)). Nonetheless, it should be noted that skin-electrode impedance measurements can differ greatly depending on the person [46] and ambient conditions such as temperature and humidity. Using the 5% PUD/PEDOT:PSS epidermal electrodes, electromyogram (figure 7(b)) and electrocardiogram (figure 7(c)) signals were recorded with recognizable ECG peaks (figure 7(d)). The properties of our printed 5% PUD/PEDOT:PSS based skin electrode are listed in table 2 alongside other printed and molded

**Table 2.** Reported epidermal electrode materials and properties including Young's modulus, electrical conductivity, skin-electrode impedance, adhesion, and printability.

| Fabrication method | Material | Modulus (MPa) | Conductivity ($S \cdot cm^{-1}$) | Skin-electrode impedance at 10 Hz ($k\Omega \cdot cm^2$) | Adhesion | References |
|---|---|---|---|---|---|---|
| Microfabrication (photolitohgraphy) | PDMS, silver microparticles | 1 | >100 | 50 | Yes | [10] |
| Inkjet printing | PEDOT:PSS (PH1000) on paper | N/A | ~240 | 3680 (1 Hz) | No | [14] |
| Molding | PEDOT:PSS (PH1000), waterborne PU, sorbitol | ~40 | ~350 | 80 | Yes | [4] |
| Screen-printing | PEDOT:PSS (PH1000), DMSO, Triton X-100, on textile | N/A | N/A | 270 | No | [15] |
| Direct-ink write printing | 5% PUD/PEDOT:PSS (PH1000), silver, on PDMS/Ecoflex | 15 | 32 | 370 (10 Hz) 1111 (1 Hz) | Yes | This work |

PEDOT:PSS-based dry electrodes reported in literature and a commercialized dry electrode fabricated using photolithography. In contrast to the inkjet-printed PEDOT:PSS electrode on paper [14], our PUD/PEDOT:PSS electrode showed superior stretchability and lower skin-electrode impedance, despite exhibiting lower conductivity. This improvement is likely due to the adhesion of the electrode creating a tighter interface with the skin, thereby eliminating air gaps at the contact region, unlike dry non-adhesive electrodes. In comparison, PEDOT:PSS electrodes have previously been combined with waterborne PU and sorbitol and displayed high electrical conductivity and low skin-electrode impedance [4]. Nonetheless, our PUD/PEDOT:PSS electrodes have a lower Young's modulus, which may be due to the lower molecular weight of PUD compared to waterborne PU. Furthermore, our formulation also provides an added benefit in that it results in a self-healing electrode, enhancing both its durability and long-term functionality. Yet another benefit of the presented electrodes is their printability. Conventional microfabrication, molding, and screen-printing require the use of a mask, mold, or stencil to define the desired patterns, whereas inkjet and direct-ink write printing techniques provide straightforward and cost-effective customization of various designs without the need for an intermediary step.

## 4. Conclusions and perspectives

In summary, we reported a printable PEDOT:PSS-based formulation characterized by light adhesion, stretchability, high conductivity, and electrical self-healing ability. As a result of studying the effects of different additives, a light adhesion of ~0.03 N $cm^{-1}$ was obtained for the 5% PUD/PEDOT:PSS films with a conductivity of approximately 30 S $cm^{-1}$ and a stretchability of 30%, stemming from PUD. Moreover, the PUD/PEDOT:PSS films demonstrated resilience to repeated strain, consistent electrical self-healing, and biocompatibility. These properties are critical for durable and reliable epidermal electrodes. Finally, to demonstrate the potential for soft electronics, we fabricated PUD/PEDOT:PSS dry electrodes using direct-ink writing. The electrodes displayed a skin-electrode impedance similar to that of commercial Ag/AgCl dry gel electrodes and successfully recorded ECG and EMG signals. The dry electrodes developed in this study feature tunable adhesion and do not apply a strong peel-off force on the skin when removed, making them suitable for continuous recordings. In addition, the PUD/PEDOT:PSS dry electrodes do not suffer from water loss, unlike conventional hydrogel-based electrodes. Therefore, these printable dry electrodes hold promising potential for healthcare monitoring. Since the PEDOT:PSS formulation is printable, this research paves the way for the development of rapidly customizable dry self-healable electrodes with tunable adhesion, electrical, and mechanical properties. Further research is needed to achieve reusable adhesives and tests for prolonged monitoring of electrophysiological signals in patients with sensitive skin such as premature infants.

## Data availability statement

The data cannot be made publicly available upon publication because they are not available in a format that is sufficiently accessible or reusable by other researchers. The data that support the findings of this study are available upon reasonable request from the authors.

## Funding

This work was supported by the Natural Sciences and Engineering Research Council of Canada (NSERC Discovery Grant RGPIN-2017-06319), Canada First (Transmedtech Institute, project 'Stretchy Electrodes' and National Defence Canada (IDEas

project CFPMN1-008), awarded to FC. P K is grateful to the Fonds de recherche du Québec—Nature et technologies (FRQNT, 316968), NSERC and Pierre Arbour foundation for a MSc scholarship. JK acknowledges the Trottier Energy Institute for a Doctoral Scholarship. J F acknowledges NSERC for a Postdoctoral Scholarship. X Z is grateful to the China Scholarship Council for a Doctoral Scholarship. Equipment and infrastructure used for this research were acquired and maintained by the Canada Foundation for Innovation and Quebec Strategic Networks (RQMP and CREPEC).

## Ethical statement

The protocol for human experiments was approved by the ethical committee of Polytechnique Montreal (approval number CER-2021-04-D).

## ORCID iDs

Pierre Kateb https://orcid.org/0000-0003-0893-4521
Jiaxin Fan https://orcid.org/0000-0001-6033-174X
Jinsil Kim https://orcid.org/0009-0001-6295-5633
Gregory A Lodygensky https://orcid.org/0000-0001-8431-4979
Fabio Cicoira https://orcid.org/0000-0002-0047-608X

## References

[1] Rossetti N, Jo'Elen H, Kateb P and Cicoira F 2021 Neural and electromyography PEDOT electrodes for invasive stimulation and recording *J. Mater. Chem. C* **9** 7243–63
[2] Abbasipour M, Kateb P, Cicoira F and Pasini D 2023 Stretchable kirigami-inspired conductive polymers for strain sensors applications *Flex. Print. Electron.* **8** 024003
[3] Petrossian G, Kateb P, Miquet-Westphal F and Cicoira F 2023 Advances in electrode materials for scalp, forehead, and ear EEG: a mini-review *ACS Appl. Bio Mater.* **6** 3019–32
[4] Zhang L *et al* 2020 Fully organic compliant dry electrodes self-adhesive to skin for long-term motion-robust epidermal biopotential monitoring *Nat. Commun.* **11** 1–13
[5] Someya T, Bao Z and Malliaras G G 2016 The rise of plastic bioelectronics *Nature* **540** 379–85
[6] Jo'Elen H, Kim C, Kateb P, Yeu J, Gagnon-Lafrenais N, Gee E and Kong Y L 2022 Flexible and stretchable printed conducting polymer devices for electrodermal activity measurements *Flex. Print. Electron.* **7** 16
[7] Tan P, Wang H, Xiao F, Lu X, Shang W, Deng X, De Vivo M and Marcia M 2022 Solution-processable, soft, self-adhesive, and conductive polymer composites for soft electronics *Nat. Commun.* **13** 1–12
[8] Zhou X, Rajeev A, Subramanian A, Li Y, Rossetti N, Natale G, Lodygensky G A and Cicoira F 2022 Self-healing, stretchable, and highly adhesive hydrogels for epidermal patch electrodes *Acta Biomater.* **139** 296–306
[9] Meziane N, Webster J, Attari M and Nimunkar A 2013 Dry electrodes for electrocardiography *Physiol. Meas.* **34** R47
[10] Stauffer F, Thielen M, Sauter C, Chardonnens S, Bachmann S, Tybrandt K, Peters C, Hierold C and Vörös J 2018 Skin conformal polymer electrodes for clinical ECG and EEG recordings *Adv. Healthcare Mater.* **7** 1700994
[11] Leenen M A, Arning V, Thiem H, Steiger J and Anselmann R 2009 Printable electronics: flexibility for the future *Phys. Status Solidi* a **206** 588–97
[12] Azimi M, Kim C-H, Fan J and Cicoira F 2023 Effect of ionic conductivity of electrolyte on printed planar and vertical organic electrochemical transistors *Faraday Discuss.* **246** 540–55
[13] Kim C-H, Azimi M, Fan J, Nagarajan H, Wang M and Cicoira F 2023 All-printed and stretchable organic electrochemical transistors using a hydrogel electrolyte *Nanoscale* **15** 3263–72
[14] Bihar E, Roberts T, Saadaoui M, Hervé T, De Graaf J B and Malliaras G G 2017 Inkjet-printed PEDOT: PSS electrodes on paper for electrocardiography *Adv. Healthcare Mater.* **6** 1601167
[15] Sinha S K, Noh Y, Reljin N, Treich G M, Hajeb-Mohammadalipour S, Guo Y, Chon K H and Sotzing G A 2017 Screen-printed PEDOT: PSS electrodes on commercial finished textiles for electrocardiography *ACS Appl. Mater. Interfaces* **9** 37524–8
[16] Fan J, Parr S, Kang S and Gupta M 2023 Point-of-care (POC) SARS-CoV-2 antigen detection using functionalized aerosol jet-printed organic electrochemical transistors (OECTs) *Nanoscale* **15** 5476–85
[17] Zhou X, Kateb P, Miquet-Westphal F, Lodygensky G A and Cicoira F 2023 Soft, conductive, and anti-freezing conducting polymer organohydrogels *Adv. Sens. Res.* 2300072
[18] Li Y, Zhang S, Hamad N, Kim K, Liu L, Lerond M and Cicoira F 2020 Tailoring the self-healing properties of conducting polymer films *Macromol. Biosci.* **20** 2000146
[19] Zhang S and Cicoira F 2017 Water-enabled healing of conducting polymer films *Adv. Mater.* **29** 1703098
[20] Su X, Wu X, Chen S, Nedumaran A M, Stephen M, Hou K, Czarny B and Leong W L 2022 A highly conducting polymer for self-healable, printable, and stretchable organic electrochemical transistor arrays and near hysteresis-free soft tactile sensors *Adv. Mater.* **34** 2200682
[21] Ye F, Li M, Ke D, Wang L and Lu Y 2019 Ultrafast self-healing and injectable conductive hydrogel for strain and pressure sensors *Adv. Mater. Technol.* **4** 1900346
[22] Taroni P J *et al* 2018 Toward stretchable self-powered sensors based on the thermoelectric response of PEDOT: PSS/polyurethane blends *Adv. Funct. Mater.* **28** 1704285
[23] He H and Ouyang J 2020 Enhancements in the mechanical stretchability and thermoelectric properties of PEDOT: PSS for flexible electronics applications *Acc. Mater. Res.* **1** 146–57
[24] Joseph J, Patel R, Wenham A and Smith J 2018 Biomedical applications of polyurethane materials and coatings *Trans. IMF* **96** 121–9
[25] Shin E J and Choi S M 2018 Advances in waterborne polyurethane-based biomaterials for biomedical applications *Novel Biomaterials for Regenerative Medicine* vol 1077 (Springer) pp 251–83
[26] Barrioni B R, de Carvalho S M, Oréfice R L, de Oliveira A A R and de Magalhães Pereira M 2015 Synthesis and characterization of biodegradable polyurethane films based on HDI with hydrolyzable crosslinked bonds and a homogeneous structure for biomedical applications *Mater. Sci. Eng.* C **52** 22–30
[27] ASTM D882–12 2012 Standard test method for tensile properties of thin plastic sheeting: ASTM International
[28] ASTM D6862–11 2016 Standard test method for 90 degree peel resistance of adhesives
[29] Makowski D, Pham T, Lau Z J, Brammer J C, Lespinasse F and Pham H 2021 NeuroKit2: a python toolbox for neurophysiological signal processing *Behav. Res. Methods* **53** 1–8
[30] Carreiras C, Alves A P, Lourenço A, Canento F, Silva H and Fred A 2018 BioSPPy: biosignal Processing in Python 2015 (available at: https://githubcom/PIA-Group/BioSPPy)

[31] Li Y, Li X, Zhang S, Liu L, Hamad N, Bobbara S R, Pasini D and Cicoira F 2020 Autonomic self-healing of PEDOT: PSS achieved via polyethylene glycol addition *Adv. Funct. Mater.* **30** 2002853
[32] He H, Zhang L, Guan X, Cheng H, Liu X, Yu S, Wei J and Ouyang J 2019 Biocompatible conductive polymers with high conductivity and high stretchability *ACS Appl. Mater. Interfaces* **11** 26185–93
[33] Hwang I, Kim H N, Seong M, Lee S H, Kang M, Yi H, Bae W G, Kwak M K and Jeong H E 2018 Multifunctional smart skin adhesive patches for advanced health care *Adv. Healthcare Mater.* **7** 1800275
[34] Kim J, Hwang Y, Jeong S, Lee S Y, Choi Y and Jung S 2018 An elastomer for epidermal electronics with adjustable adhesion force and stretchability obtained via a reverse-micelle-induced process *J. Mater. Chem.* C **6** 2210–5
[35] Waring M, Bielfeldt S and Brandt M 2009 Skin adhesion properties of three dressings used for acute wounds *Wounds UK* **5** 22–31
[36] Wang L, Wang J, Fan C, Xu T and Zhang X 2022 Skin-like hydrogel-elastomer based electrochemical device for comfortable wearable biofluid monitoring *Chem. Eng. J.* **455** 140609
[37] Kalra A, Lowe A and Al-Jumaily A 2016 Mechanical behaviour of skin: a review *J. Mater. Sci. Eng.* **5** 1000254
[38] Kayser L V and Lipomi D J 2019 Stretchable conductive polymers and composites based on PEDOT and PEDOT: PSS *Adv. Mater.* **31** 1806133
[39] Lo L-W, Zhao J, Wan H, Wang Y, Chakrabartty S and Wang C 2021 An inkjet-printed PEDOT: PSS-based stretchable conductor for wearable health monitoring device applications *ACS Appl. Mater. Interfaces* **13** 21693–702
[40] Timpanaro S, Kemerink M, Touwslager F, De Kok M and Schrader S 2004 Morphology and conductivity of PEDOT/PSS films studied by scanning–tunneling microscopy *Chem. Phys. Lett.* **394** 339–43
[41] Wang T, Qi Y, Xu J, Hu X and Chen P 2005 Effects of poly (ethylene glycol) on electrical conductivity of poly (3, 4-ethylenedioxythiophene)–poly (styrenesulfonic acid) film *Appl. Surf. Sci.* **250** 188–94
[42] Li Y, Zhou X, Sarkar B, Gagnon-Lafrenais N and Cicoira F 2022 Recent progresses on self-healable conducting polymers *Adv. Mater.* **34** e2108932
[43] Wei Q, Mukaida M, Ding W and Ishida T 2018 Humidity control in a closed system utilizing conducting polymers *RSC Adv.* **8** 12540–6
[44] Roig F, Dantras E, Dandurand J and Lacabanne C 2011 Influence of hydrogen bonds on glass transition and dielectric relaxations of cellulose *J. Phys. D: Appl. Phys.* **44** 045403
[45] 10993–5 I 2009 Biological evaluation of medical devices—part 5: tests for in vitro cytotoxicity (IOS)
[46] Yang L, Li H, Ding J, Li W, Dong X, Wen Z and Shi X 2018 Optimal combination of electrodes and conductive gels for brain electrical impedance tomography *Biomed. Eng. Online* **17** 1–22